Expanded View Figures

Figure EV1. Expression of a subset of ER-resident transmembrane proteins can induce autophagy of ER whorls.

A Electron micrograph of a yeast cell treated with DTT for 3 h. White arrows indicate ER whorls in the vacuole. Cy, cytosol; N, nucleus; V, vacuole.

B Fluorescence images of cells expressing the ER marker Sec63-GFP. Cells were left untreated or treated with DTT for 3 h. DTT induces expansion of the peripheral ER and formation of ER extensions into the cytosol, but no structures resembling whorls are visible. Scale bar: 2 μm.

C Schematic representation of GFP-tagged transmembrane proteins used.

D Western blot of Pho8 from wild-type cells and cells expressing GFP-Pho8 under the *GAL* or *GPD* promoter, or monomeric GFP(L221K)-Pho8 (mGFP-Pho8) under the *GPD* promoter. Pgk1 served as a loading control. Note that *GAL*- and *GPD*-driven expression of GFP-Pho8 resulted in similar levels.

E Fluorescence images of CMAC-stained cells expressing the ER marker Sec63-mCherry and *GPD* promoter-driven Pho8 fused to regular GFP or monomeric GFP(L221K) (mGFP). GFP-Pho8 forms ER stretches and rings that can be taken up into the vacuole. mGFP-Pho8 does not alter the structure of the ER and is transported to the vacuole membrane. Scale bar: 2 μm.

F Fluorescence images of CMAC-stained cells expressing *GAL* promoter-driven GFP-Pho8 and the ER markers Sec61-mCherry, mCherry-Ubc6, or dsRed-HDEL. GFP-Pho8 and the ER markers highlight ring structures inside CMAC-stained vacuoles. Scale bar: 2 μm.

G Fluorescence images of CMAC-stained cells expressing Sec63-mCherry and either Hmg1-GFP, GFP-Cyb5, or P450M4-GFP under the control of the *GAL* promoter. Scale bar: 2 μm.

Source data are available online for this figure.

© 2019 The Authors

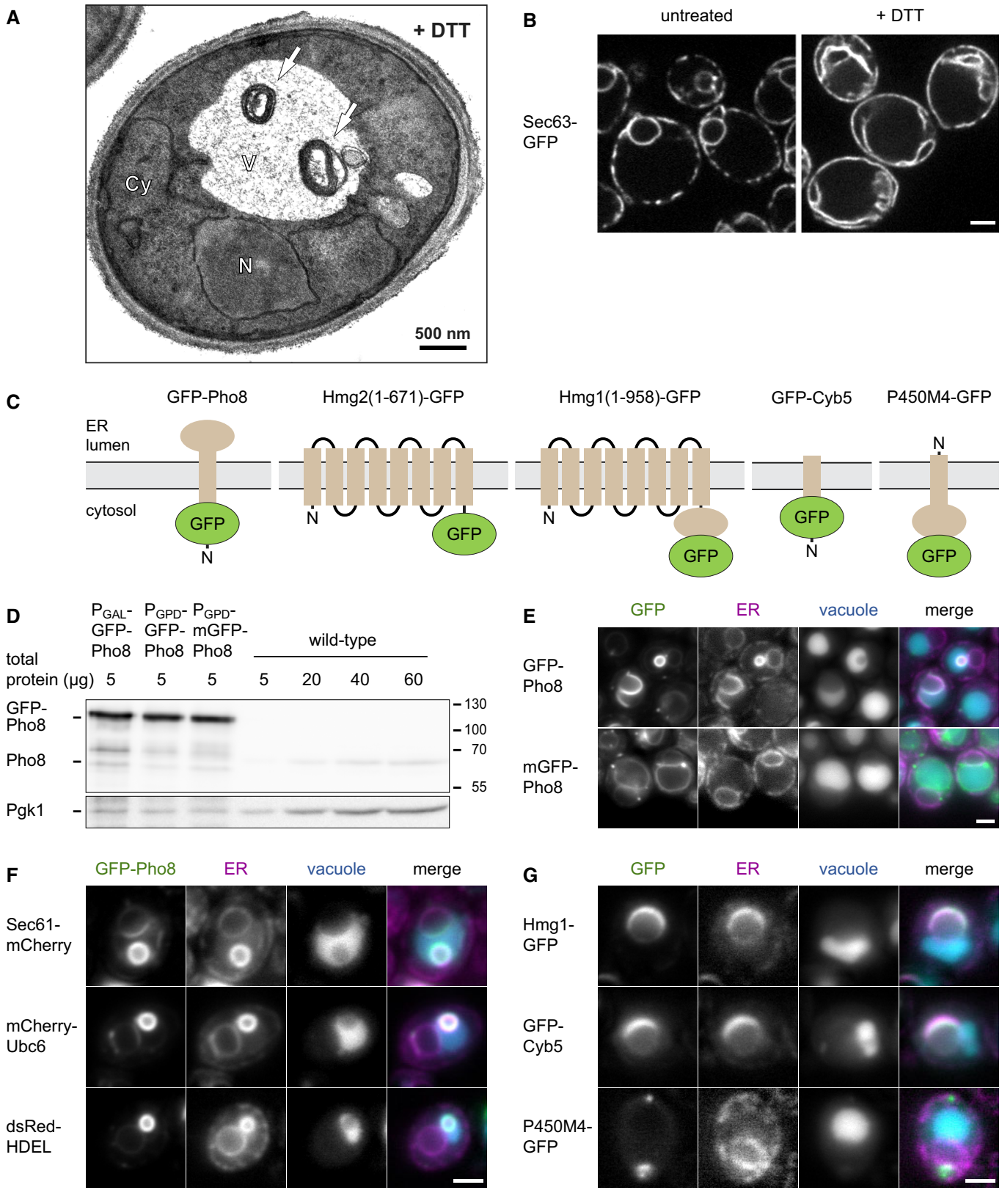

Figure EV1.

Figure EV2. ER whorls arise from ER stacks and undergo microautophagy.

A Conversion times of bent stacks into vacuolar whorls. $n = 29$.

B Fluorescence images of a cell expressing GFP-Pho8 and stained with the vacuole membrane dye FM4-64. The whorl is completely surrounded by vacuole membrane but has an opening (arrow). Scale bar: 2 μm.

C Individual frames from time-lapse imaging of a cell expressing GFP-Pho8 and stained with the vacuole dye CMAC. The image sequence shows the conversion of a peripheral stack into a cytosolic whorl. Numbers indicate the time in minutes after the start of the image sequence. Scale bar: 2 μm.

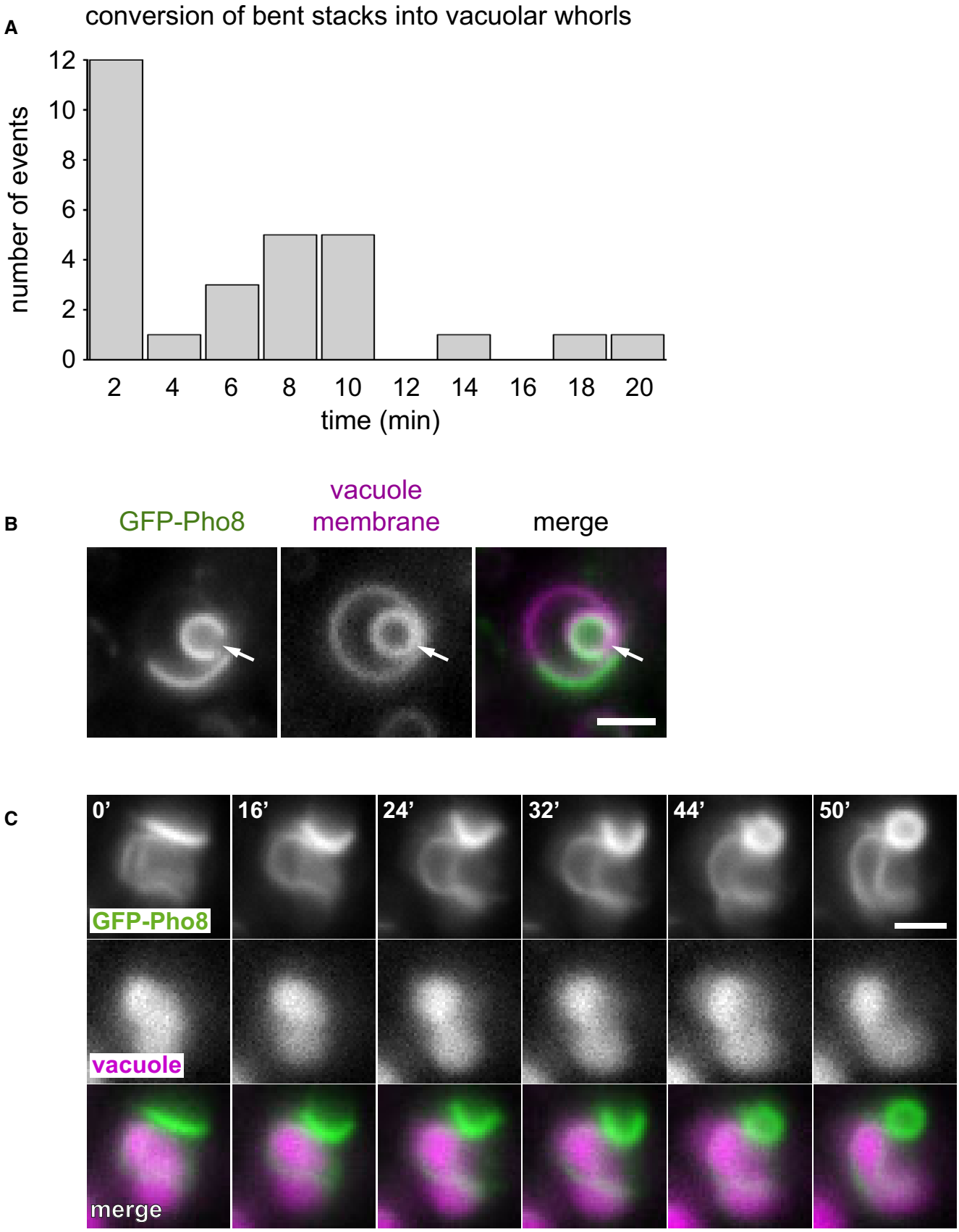

Figure EV2.

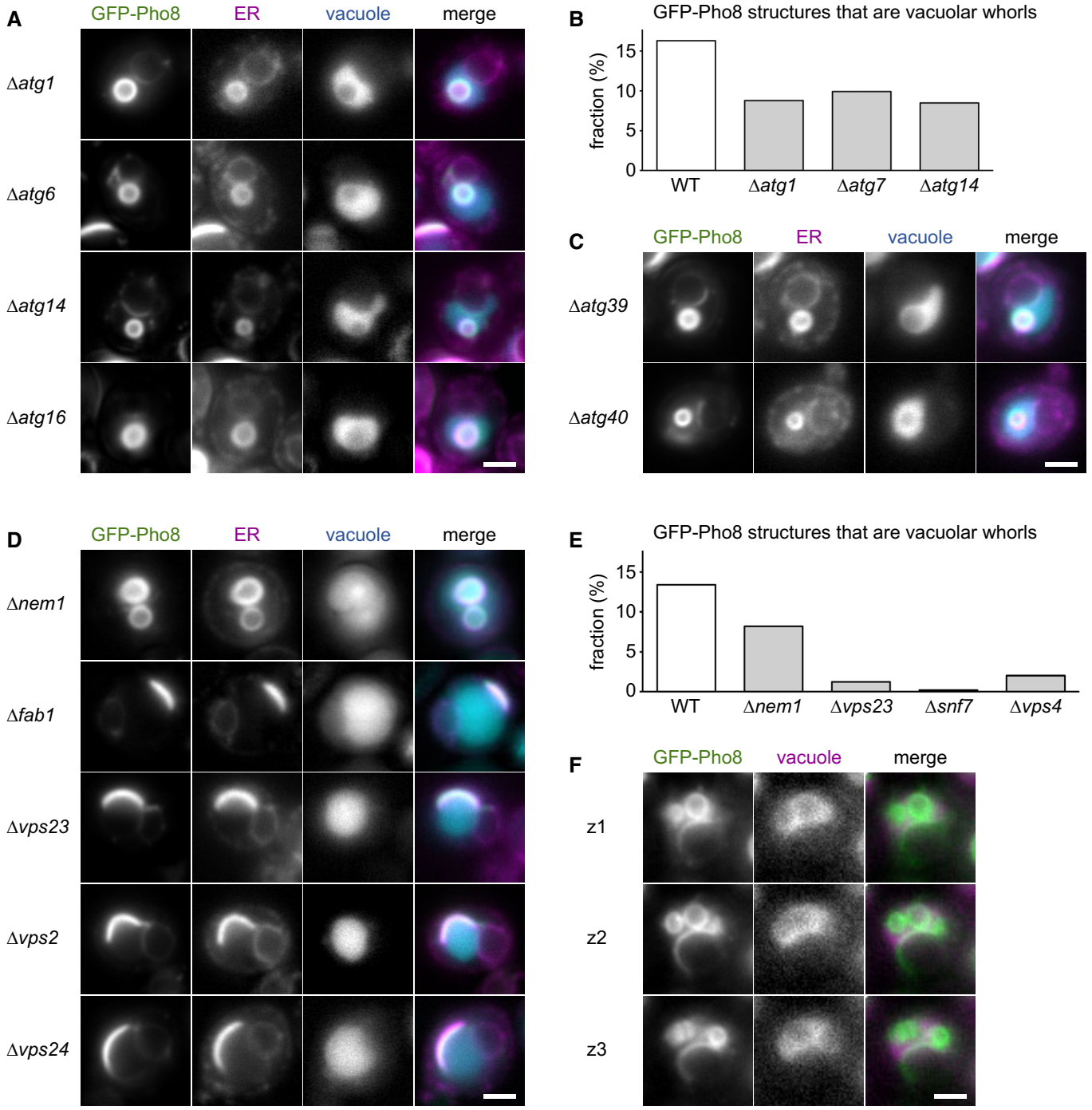

Figure EV3. The Nem1-Spo7 complex and ESCRTs are key components for micro-ER-phagy.

A Fluorescence images of Δ*atg1*, Δ*atg6*, Δ*atg14*, and Δ*atg16* cells expressing GFP-Pho8 and the ER marker Sec63-mCherry and stained with CMAC to label the vacuole. Scale bar: 2 μm.

B Fraction of GFP-Pho8 structures that are vacuolar whorls in wild-type (WT), Δ*atg1*, Δ*atg7*, and Δ*atg14* cells. Core autophagy machinery mutants are still capable of autophagy of GFP-Pho8 whorls.

C Fluorescence images of Δ*atg39* and Δ*atg40* cells expressing GFP-Pho8 and the ER marker Sec63-mCherry and stained with CMAC to label the vacuole. Scale bar: 2 μm.

D Fluorescence images of Δ*nem1*, Δ*fab1*, Δ*vps23*, Δ*vps2*, and Δ*vps24* cells expressing GFP-Pho8 and the ER marker Sec63-mCherry and stained with CMAC to label the vacuole. Note that the whorls in Δ*nem1* cells contain CMAC. Scale bar: 2 μm.

E Fraction of GFP-Pho8 structures that are vacuolar whorls in wild-type (WT), Δ*nem1*, Δ*vps23*, Δ*snf7*, and Δ*vps4* cells.

F Individual planes from a z-stack of a Δ*nem1* cell showing multiple whorls in the same vacuole. Scale bar: 2 μm.

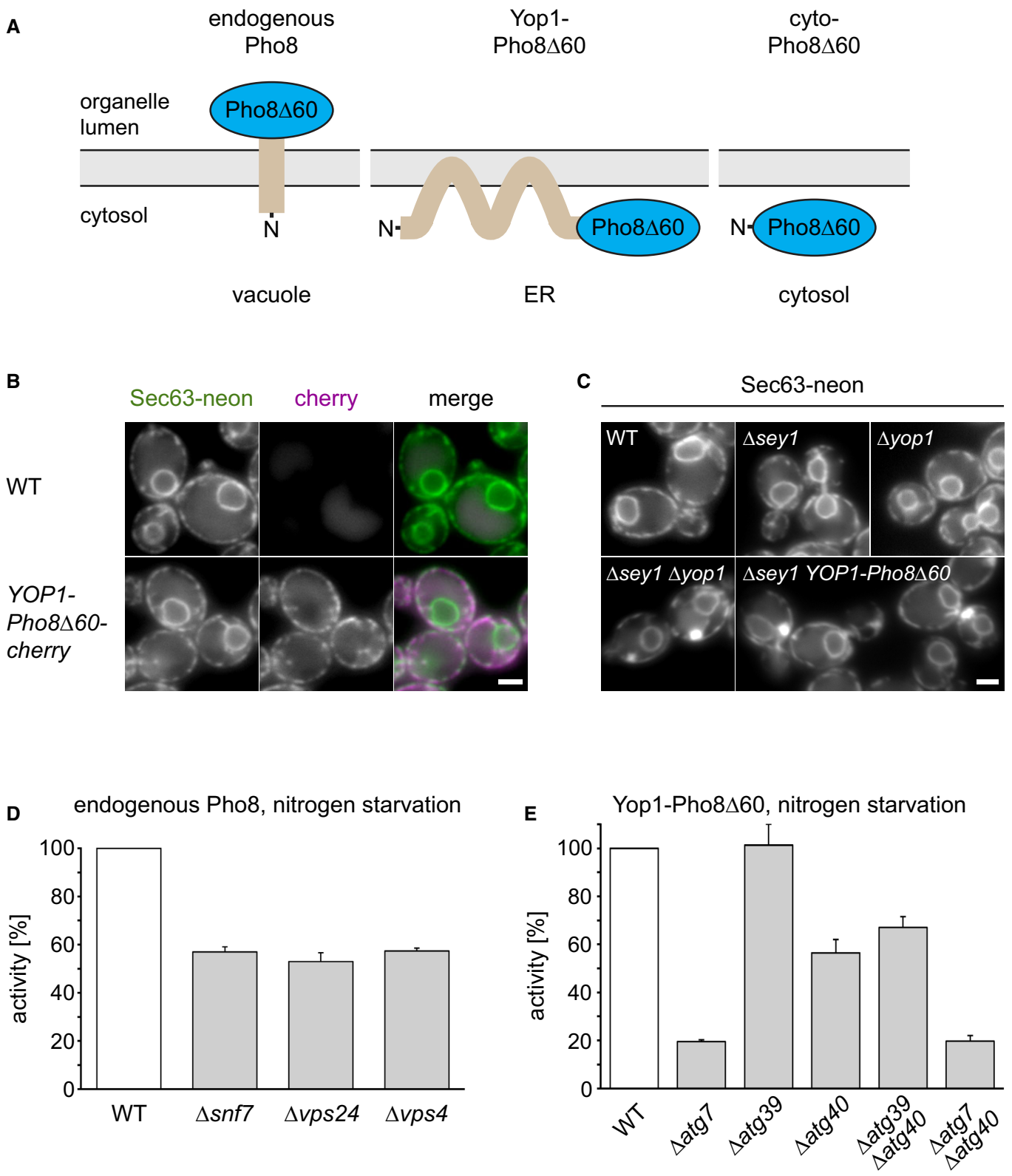

Figure EV4.

Figure EV4. Macro- and micro-ER-phagy are parallel pathways with distinct molecular requirements.

A Schematic representation of Pho8-based autophagy reporters.
B Fluorescence images of wild-type and *YOP1-Pho8Δ60-mCherry* cells expressing Sec63-mNeonGreen. Yop1-Pho8Δ60-mCherry localizes to the peripheral ER and does not disturb overall ER morphology. Scale bar: 2 μm.
C Fluorescence images of cells of the indicated genotypes expressing Sec63-mNeonGreen. Δ*sey1* Δ*yop1* cells have a disrupted ER morphology (Hu *et al*, 2009). Tagging of *YOP1* with Pho8Δ60 in a Δ*sey1* background results in the same ER morphology phenotype as combined deletion of *SEY1* and *YOP1*, indicating that Yop1-Pho8Δ60 is non-functional. Scale bar: 2 μm.
D Relative activity of endogenous Pho8 after nitrogen starvation. Mean + SEM, $n = 3$.
E Relative activity of the ER-phagy reporter Yop1-Pho8Δ60 after nitrogen starvation. *ATG40* is involved in autophagy of Yop1-Pho8Δ60 and is epistatic with *ATG7*. Mean + SEM, $n \geq 3$.

Figure EV5. ESCRT machinery mediates vacuole membrane dynamics during micro-ER-phagy of GFP-Pho8 structures.

A GFP-Pho8 expression levels as measured by flow cytometry. Mean + SEM, $n \geq 3$.
B Individual frames from time-lapse imaging of a Δ*ups4* mutant expressing GFP-Pho8 and stained with the vacuole membrane dye FM4-64. Numbers indicate the time in minutes after the start of the image sequence. Scale bar: 2 μm.
C Fluorescence images of wild-type (WT) and Δ*snf7* cells expressing GFP-Pho8 and the ESCRT cargo cherry-CPS. Deletion of *SNF7* leads to accumulation of cherry-CPS in enlarged late endosomes near the vacuole, but there is no co-localization with vacuole-associated GFP-Pho8 stacks. Scale bar: 2 μm.
D Snf7-mNeonGreen expression levels as measured by flow cytometry upon expression from the *SNF7* or *VPS24* promoter.
E Localization of the ESCRT cargo cherry-CPS in wild-type and Δ*snf7* cells in the absence or presence of Snf7-mNeonGreen. Snf7-mNeonGreen does not interfere with cherry-CPS transport into the vacuole in WT cells and does not rescue defective cherry-CPS transport in Δ*snf7* cells. Scale bar: 2 μm.
F Relative activity of the ER-phagy reporter Yop1-Pho8Δ60 in tunicamycin-treated cells. Mean + SEM, $n = 3$. Snf7-mNeonGreen has no effect on micro-ER-phagy activity in Δ*atg7* or Δ*atg7* Δ*snf7* cells.
G Duration of Snf7 appearance at vacuolar whorls. $t = 0$ indicates whorls for which no closely apposed Snf7 punctum could be detected. Twenty-five whorls were analyzed, and a Snf7 punctum was observed for 19 (76%). Six whorls were visited by Snf7 multiple times, resulting in a total of 28 recruitment events.

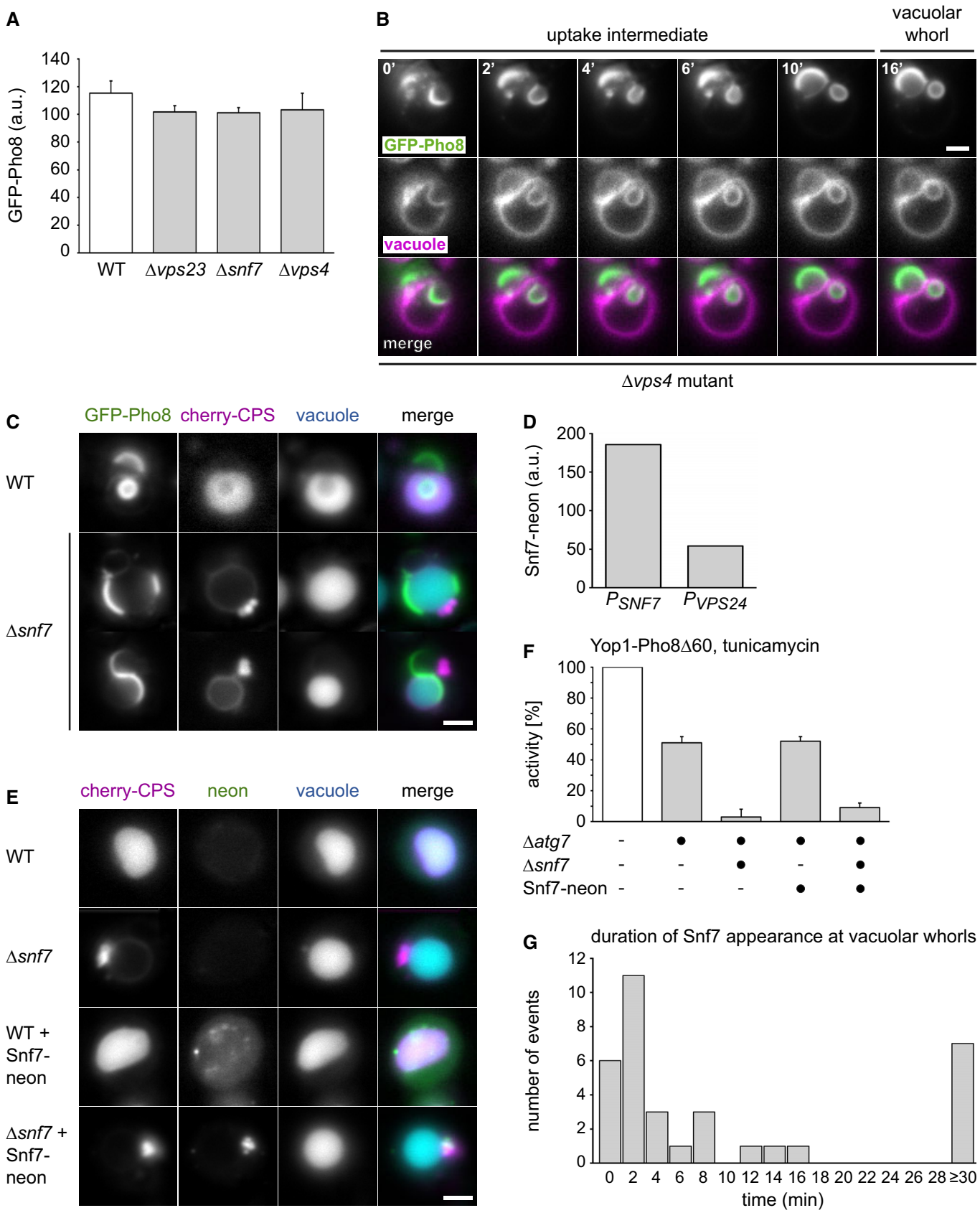

Figure EV5.